Hindawi Publishing Corporation
Journal of Spectroscopy
Volume 2014, Article ID 748468, 14 pages
http://dx.doi.org/10.1155/2014/748468

Research Article

Physicochemical Analysis and Molecular Modeling of the Fosinopril β-Cyclodextrin Inclusion Complex

Lucreţia Udrescu,[1,2] Laura Sbârcea,[1] Adriana Fulias,[1] Ionuţ Ledeţi,[1] Gabriela Vlase,[3] Paul Barvinschi,[4] and Ludovic Kurunczi[2]

[1] *Faculty of Pharmacy, University of Medicine and Pharmacy, 300041 Timişoara, Romania*
[2] *Institute of Chemistry Timişoara of the Romanian Academy, 300223 Timişoara, Romania*
[3] *Research Center for Thermal Analysis in Environmental Problems, West University of Timişoara, 300115 Timişoara, Romania*
[4] *Faculty of Physics, West University of Timişoara, 300223 Timişoara, Romania*

Correspondence should be addressed to Lucreţia Udrescu; udrescu.lucretia@umft.ro and Laura Sbârcea; sbarcea.laura@umft.ro

Received 24 July 2014; Revised 10 October 2014; Accepted 11 October 2014; Published 6 November 2014

Academic Editor: Eugen Culea

This research investigates the interaction between fosinopril sodium (FOS) and beta-cyclodextrin (β-CD) in aqueous solution and in solid state, in order to prove the formation of an inclusion complex between the two components. The stoichiometry of the inclusion complex was found as 1:1 by employing continuous variation method in UV. The formation constant was calculated as 278.93 M^{-1} using Benesi-Hildebrand equation. The kneaded product (KP) and the physical mixture (PM) were further experimentally examined, using FTIR, powder X-ray diffractometry, and thermal analysis. The results confirm that the physicochemical properties of the FOS/β-CD KP are different from FOS and that the kneading method leads to formation of solid state inclusion complex between FOS and β-CD. Structural studies of the FOS/β-CD were carried out using molecular modeling techniques, in order to explain the complexation mechanism and the host-guest geometry.

1. Introduction

Cyclodextrins are cyclic oligosaccharides that have the ability to form inclusion complexes with small molecules or with hydrophobic moiety of larger molecules [1]. β-CD is the heptacyclic oligomer of glucose, having the smallest water solubility at 25°C from all natural cyclodextrins. At the same time, β-CD is the most used natural cyclodextrin in pharmaceutical applications, due to its properties which allow for increasing the drug solubility in aqueous solution, improving the bioavailability, masking the inappropriate organoleptic properties such as odor or taste, protecting the included substance from oxidation, and losing through volatilization.

Biocompatibility is an essential condition for any drug excipient, and the toxicological studies indicate that cyclodextrin's biocompatibility depends on the route of administration as well as on the particular chemical structure; β-CD is well tolerated in humans after oral administration [2]; therefore it is mainly used in oral dosage forms [3, 4].

Fosinopril sodium, chemically named sodium (2S,4S)-4-cyclohexyl-1-(2-{[2-methyl-1-(propanoyloxy)propoxy](4-phenylbutyl)phosphoryl}acetyl)pyrrolidine-2-carboxylate (presented in Figure 1(a)), is the only phosphinic acid derivative among the angiotensin converting enzyme (ACE) inhibitors class. It is used for the treatment of essential hypertension, congestive heart failure, diabetic nephropathy, and postmyocardial infarction [5].

FOS is an ester prodrug, which becomes active in vivo after being hydrolyzed to the active diacid form, namely, fosinoprilat; see Figure 1(b). Fosinopril sodium is highly lipophilic (n-octanol/water ratio of 6.19 [6]), as well as the active form, fosinoprilat (log P = 3.70 [7]).

The oral absorption of FOS differs depending on its pharmaceutical dosage form, ranging between 32% (solution doses) and 36% (capsule doses). After the hydrolysis, the

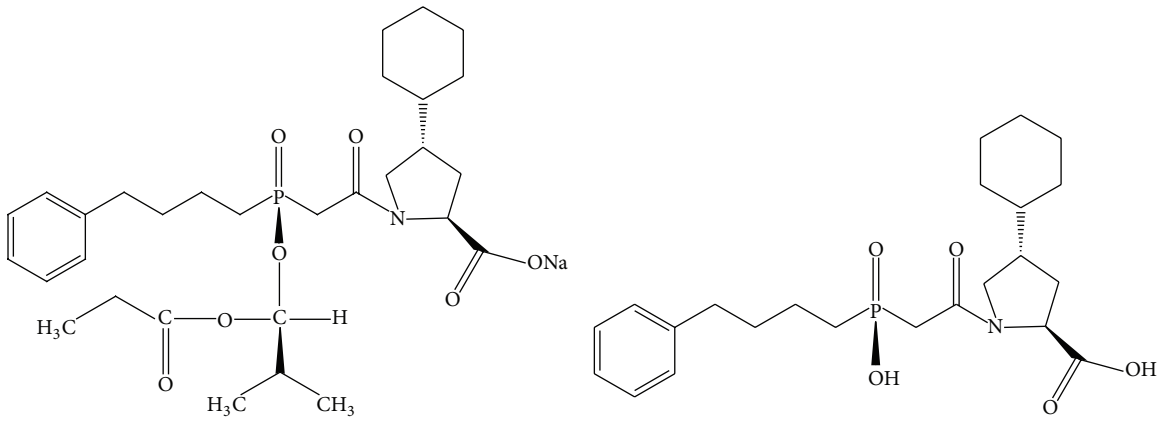

Figure 1: Chemical structure of (a) fosinopril sodium and (b) fosinoprilat.

bioavailability of oral fosinoprilat is averaged as 25% and 29% for solution and capsule doses, respectively [5].

FOS is a white to almost white crystalline powder; it is freely soluble in water, sparingly soluble in anhydrous ethanol, and practically insoluble in hexane [8, 9]. The drug absorption from the administration site into the blood stream is strongly swayed by the drug solubility: a low solubility leads to a poor absorption [4, 10]. Wang et al. studied the properties of fosinopril sodium in aqueous media and demonstrated that the hydrophobic interactions create incentives for the occurrence of micellar aggregates, with a critical micelle concentration (cmc) of approximately 1.5 mg/mL, and with an average diameter of approximately 150 nm of the micellar aggregate, at concentrations above the cmc. The surface activity and the aggregation behavior of fosinopril could cause its concentration-dependent stability in aqueous solution, unanticipated solubility decrease in the presence of metal ions, also diminished absorption in clinical trials [11].

The feasibility of cyclodextrin complexation is mainly driven by the low bioavailability of the drug, which in turn is determined by the low solubility and the crystalline state. As such, the fact that the cyclodextrin-drug inclusion complex is isolated as amorphous or microcrystalline powder [3] contributes to both higher solubility and improved bioavailability [12].

Another issue is that of damaging interaction between FOS and magnesium ions in tablet formulations lubricated with magnesium stearate [13]. The molecular level drug encapsulation within cyclodextrin cavity prevents the interaction with this excipient, improving the FOS stability in tablets dosage form which contain magnesium stearate as lubricant [3, 13].

Up to date, there are only few studies focused on FOS properties and its cyclodextrin inclusion complexes that have been reported [9, 14–16]. In this context, the main contributions of this paper are as follows.

(1) We report for the first time the interaction between FOS and β-CD in water, and we also provide the stability constant value of the FOS/β-CD inclusion complex, in water, at 25°C.

(2) The water solubility profile of FOS, at 25°C, is enhanced as a result of employing the kneading method for preparing the FOS/β-CD inclusion complex.

(3) An elaborated molecular modeling of the inclusion complex is thoroughly described, so that important aspects regarding the formation process and the geometry are clarified.

2. Materials and Methods

2.1. Materials. Fosinopril sodium was a gift sample from Terapia-Ranbaxy (Cluj-Napoca, Romania) and it was used without further purification. β-cyclodextrin (molar mass 1135 g/mol) was obtained from Cyclolab R&D Ltd. (Budapest, Hungary). The substances were used as received. All other chemicals and reagents were of analytical grade. All experiments were carried out using ultrapure water.

2.2. Stoichiometry Determination Using Job's Plot Method. The stoichiometry of the inclusion complex was determined by applying the continuous variation from Job's method [17, 18]. Equimolar $0.8 \cdot 10^{-4}$ M solutions of FOS and β-CD were mixed in volumetric flasks to a standard volume of 10 mL (1 mL : 9 mL; 2 mL : 8 mL; and so on), varying the molar ratio, while the total concentration of the species was held constant. An analogous dilution set of the FOS stock solution was carried out using ultrapure water.

After stirring for 24 hours, at the room temperature, the absorbance for all solutions was measured at 208 nm (Figure 2(a)), using 1 cm quartz cells, and then the difference between the absorbance in the absence and in the presence of β-CD was calculated as $\Delta A = A_0 - A$. The ΔA values were plotted against mole fractions R, where R = [FOS]/{[FOS] + [β-CD]} (see Figure 2(b)).

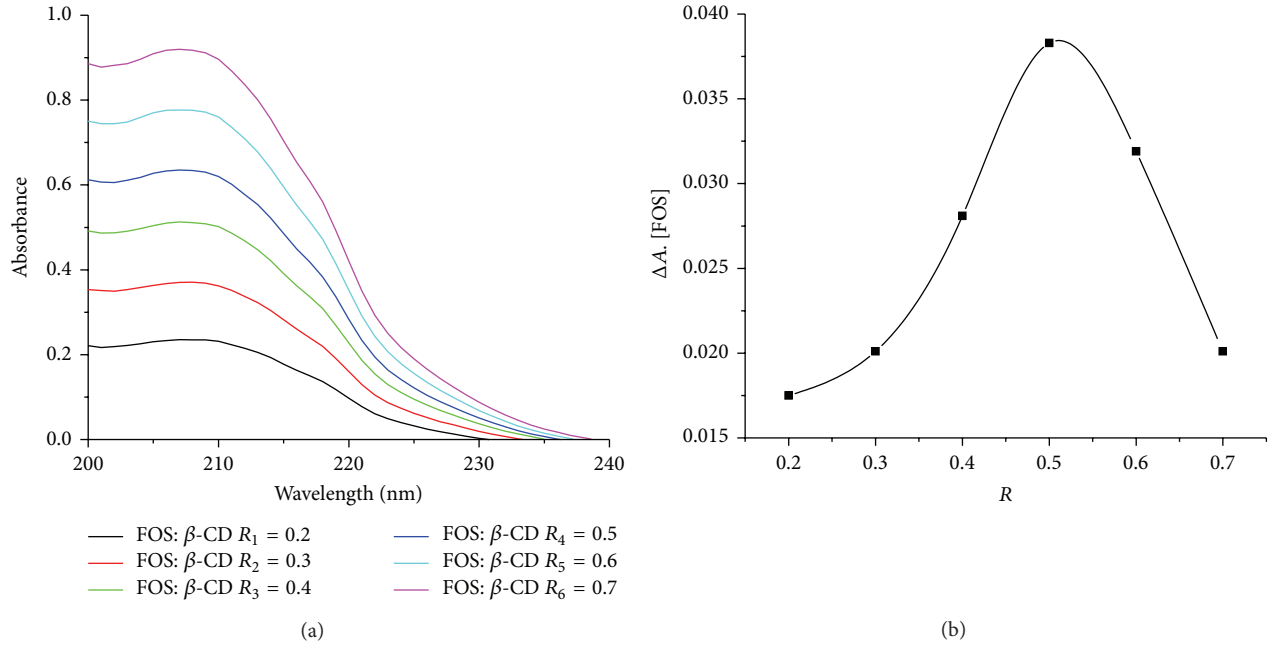

Figure 2: (a) UV spectra of aqueous solution of FOS and β-CD mixed in variable molar ratio R; (b) Job's plot for different molar ratios of FOS and β-CD from absorbance measurements.

2.3. Binding Constant Determination of the Inclusion Complex. The absorbance measurements were performed for FOS under complexation-free conditions and in the presence of growing concentration of β-CD. Thus, the concentration of FOS was kept constant at 0.1 mM and the β-CD concentration was varied from 0 to 4.5 mM. All the absorption spectra were collected in the range of 200–250 nm, using 1 cm quartz cells. The calculation of the stability constant uses the change of the absorbance at the maximum wavelength of 208 nm for FOS as a function of β-CD concentration.

The binding constant of FOS/β-CD inclusion complex was determined by Benesi-Hildebrand equation [17, 19]:

$$\frac{1}{\Delta A} = \frac{1}{[\text{FOS}] \cdot [\beta\text{-CD}] \cdot \Delta\varepsilon \cdot K_s} + \frac{1}{\Delta\varepsilon \cdot [\text{FOS}]}. \quad (1)$$

2.4. Standard Curve of FOS. A set of FOS aqueous solutions were prepared, with concentrations ranging between 4.88 and 39.07 μg/mL. The absorbance was recorded at 208 nm in UV at 25°C in order to perform a standard curve plotting concentration (C, μg/mL) as x-coordinate and absorbance A as y-coordinate. The consequently found standard curve of FOS is characterized by the equation $A = 0.0274 \cdot C + 0.0027$, with $R = 0.9999$.

2.5. Preparation of the Solid-State Binary Systems

2.5.1. Preparation of the FOS/β-CD Kneaded Product. The accurate weight of β-CD for a 1 : 1 molar ratio FOS : β-CD was triturated with an appropriate quantity of water at the ambient temperature for 10 minutes, up to homogenization. Then FOS was slowly added to the paste. While grinding, a small quantity of 1 : 1 v/v ethanol/water was blended with the mixture, in order to assist the dissolution of the drug. The paste was kneaded for 1 hour. During this process, an appropriate quantity of 1 : 1 v/v ethanol/water was added for maintaining a suitable paste consistency. The paste that was rendered with this process was dried in the oven at 40°C for 24 hours. Then, the dried kneaded product, named FOS/β-CD KP, was pulverized and passed through a 75 μm size sieve.

2.5.2. Preparation of the FOS/β-CD Physical Mixture. The stoichiometric quantities of β-CD and FOS corresponding to a 1 : 1 molar ratio were gently mixed in a mortar, at the ambient temperature for 10 minutes, in order to obtain a homogenous blend. Thus, a physical mixture consisting of FOS and β-CD at the same 1 : 1 molar ratio as the kneaded product was obtained—FOS/β-CD PM—and then used for comparison with the FOS/β-CD KP physicochemical properties.

2.6. Characterization of the Solid-State Complexes

2.6.1. Fourier-Transformed Infrared Spectroscopy (FTIR). FTIR spectra were achieved on a Jasco FT/IR 410 spectrometer, at the room temperature. Each spectrum represents 16 coadded scans, achieved at a spectral resolution of 1 cm^{-1}, in the wavenumber range 4000–400 cm^{-1}. The samples were processed using KBr pellets technique. The FTIR spectrum of the FOS/β-CD KP was compared with those of FOS, β-CD, and their physical mixture. In order to improve assessment of the position, height, and area of the bands, the recorded FTIR spectra were baseline corrected using the two-point line method in Spectra Manager Version 1.50.00 (Jasco Corporation). The same protocol was used for all analyzed

samples, in order to assure the reproducibility of the results and to facilitate the comparative analysis of all spectra.

2.6.2. Thermal Analysis. The inclusion complex between FOS and β-CD, as obtained with the kneading method, was confirmed by performing thermal analysis. To this end, a simultaneous TGA/DTA instrument from Perkin-Elmer DIAMOND was used. In these experiments, the samples of about 3 mg were placed in the aluminum crucibles. For determining the heat effects, the DTA curves (in μV) were changed with the heat flow curves (in mW); therefore the peak area corresponds to an energy expressed in kJ/mol. The thermal behavior of the substances were studied under air atmosphere, at a flow rate of 100 mL/min and the experiments were conducted under nonisothermal conditions by increasing the ambient temperature up to 500°C, with a constant heating rate of 10°C/min.

2.6.3. Powder X-Ray Diffractometry (PXRD). XRD studies of the pure substances (FOS and β-CD) and of their binary systems (PM and KP) were performed using a Bruker D8 Advance powder X-ray diffractometer, in the range of 5–45° angular domain (2θ), with CuK radiation generated at 40 mA, 40 kV, and a Ni filter.

2.7. Solubility Profile of the Kneaded Product. An excess amount of FOS/β-CD was placed in 2 mL of distilled water, so as to obtain a saturated solution. The mixture was shaken for 24 h, at 25°C, afterwards the insoluble substance was removed by filtration using 0.45 μm cellulose acetate filter. The clear supernatant was properly diluted and its absorbance was measured at 208 nm in UV, at 25°C. The residue dosing was performed by means of the standard FOS curve.

2.8. Molecular Modeling. All the calculation procedures were performed using the HyperChem program package (HyperChem 7.5 Release for Windows, HyperCube, Gainsville, Florida, USA). The starting structures used in these calculations were the crystal structures of fosinopril sodium [20, 21] and of β-cyclodextrin 10.41-hydrate [22, 23].

To find the preliminary, approximately correct position of the guest (FOS) molecule in the β-CD cavity, a molecular mechanics method was used, involving the MM+ force field. The water molecules were eliminated from the β-CD structure file. The next step was the insertion of FOS molecule in the empty host hollow. For this purpose, the third inertial axis (the cavity axis) of the β-CD was made collinear with the first inertial axis (the longest) of the FOS molecule. Along this line, the FOS was pushed gradually into the β-CD cavity with the phenyl ring oriented toward the wider rim, as for the most stable complex obtained for enalapril [24]. At each step, a complete MM+ geometry optimization was performed. The starting geometries of the molecules used in this process were those of the PM3 optimized crystalline structures. The PM3 method performs better than other semiempirical methods on O–H$\cdots$O hydrogen bond networks [25] and generates an improved description of the steric interaction effects [26].

The crystal structure of FOS molecule is relatively close to the cis conformation of Liu et al. [27], which in methanol solution is an extended form; thus the hydrophobic groups are located remotely from one another. In its crystalline state, taken from CCDC (code TUHMOY), the adjacent molecules, besides a strong Na–O bonds network, establish van der Waals interactions between the edges of the phenyl rings and the neighboring isopropyl CH_3 groups from another molecule, as well as between adjoining cyclohexyl moieties from the aligned molecules.

The binding energy was calculated by extracting the sum of MM+ energies of the free FOS and β-CD from the energy of the complex. The potentially best complex can be identified by consulting the step by step evolution of the MM+ binding energy. For the structure corresponding to the most favorable binding energy, the semiempirical PM3 quantum chemical method was run in order to obtain more reliable structures and energies (heats of formation). The SCF convergence limit of 10^{-5} and a RMS gradient of 10^{-2} kcal/Å mol were used, and the optimization was performed, by involving the Polak-Ribiere conjugate gradient method. To this end, the Na atom semiempirical parameters proposed by [28] were implemented in the HyperChem package. The final, optimized equilibrium structures were validated by harmonic frequency calculations. The PM3 method was also used in the application of the conformational search module of the HyperChem package, in the attempts to identify the conformation corresponding to the absolute minimum for the FOS molecule.

3. Results and Discussion

3.1. Job's Plot Method. According to the method of continuous variation, the maximum concentration of the complex corresponds to the molar ratio R that indicates the complexation stoichiometry. This was identified when the absorbance (a physical parameter which is directly related to the complex concentration) was measured for a series of samples having continuously varied molar fraction of its components, as presented in Figure 2(a) [17, 18].

In Figure 2(b) the maximum absorbance variation ΔA of FOS was observed for $R = 0.5$, thus indicating that the stoichiometry is 1 : 1, which is consistent with the stoichiometry suggested by the phase solubility study from our previous work [16].

3.2. Stability Constant Determination. The Benesi-Hildebrand method is one of the most common strategies for determining association constants based on absorption spectra [17, 18].

The absorbance values were collected before and after the formation of the FOS/β-CD inclusion complex (see Figure 3(a)). Then, the variation of the absorbance $\Delta A = A - A_0$ was calculated as the difference between the FOS absorbance at different β-CD concentrations and the pure FOS absorbance before the interaction, at 208 nm. The stability constant of FOS/β-CD inclusion complex was calculated using (1), rendering a linear relationship

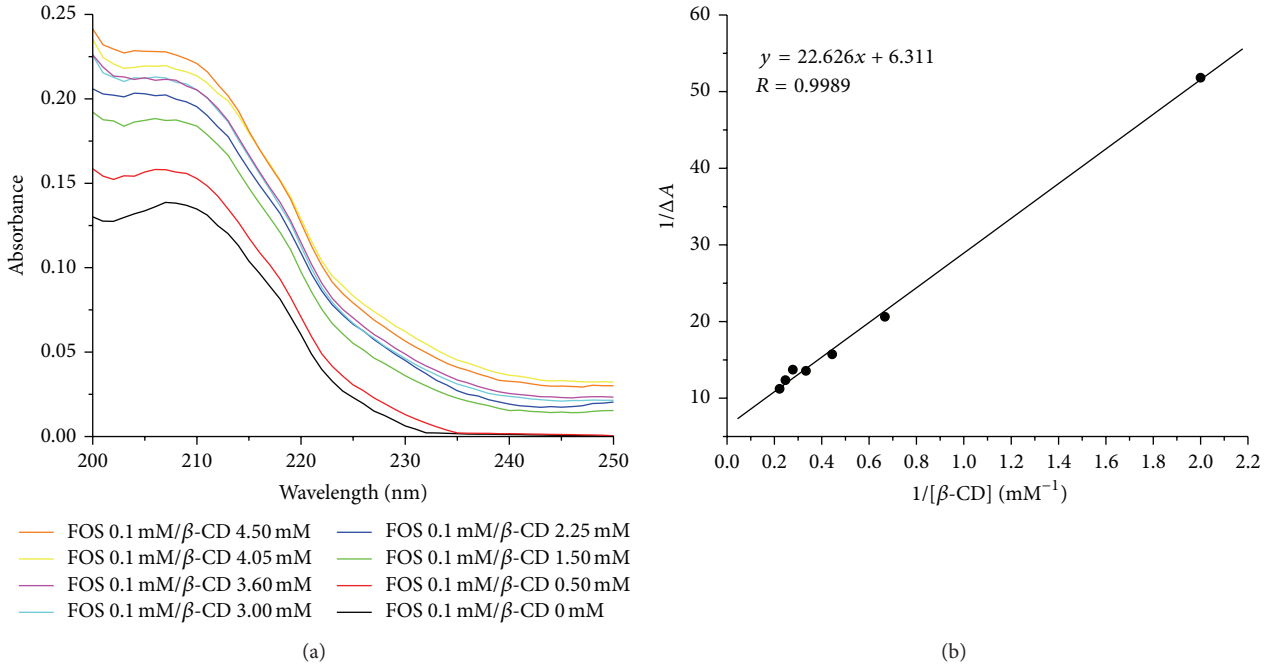

Figure 3: (a) Ultraviolet spectra of pure Fos and Fos/β-CD inclusion complex in presence of increasing β-CD concentration; (b) Benesi-Hildebrand linear plot for $1/\Delta A$ versus $1/\beta$-CD.

in $1/\Delta A$ versus $1/[\beta\text{-CD}]$ plot, as shown in Figure 3(b). By dividing the intercept with the slope of the straight line in the Benesi-Hildebrand double-reciprocal plot, K_s is calculated as 278.93 M^{-1}.

3.3. FTIR Analysis. The FTIR spectra of FOS, β-CD, along with their physical mixture and kneaded product are shown in Figure 4. For the parent molecules (see Figures 4(a) and 4(c)) the most characteristic absorbances are labeled, but in our analysis concerning the KP and PM products, only the group frequencies which are not common to FOS and β-CD structures will be used (which were also highlighted by the corresponding labels).

The spectrum of FOS, as presented in Figures 4(a) and 4(c), is characterized by the presence of the carboxyl, amide, and ester groups, which rise intense absorption peaks at 1601 cm^{-1}, 1624 cm^{-1}, and 1759 cm^{-1}, entailed by the C=O stretching vibration [29], as shown in Figure 4(a). The peak at 1454 cm^{-1} indicates the C–N stretching vibration from FOS proline ring [30]. The FOS phenyl ring presence is proven both by the weak C_{ar}–H stretching vibrations from 3000–3150 cm^{-1} region and by the out-of-plane vibration which appears at 557 cm^{-1}. The CH_3 asymmetric stretching appears at 2981 cm^{-1}. Also the CH_3 groups (ethyl, i-propyl) and their linkage with the molecular skeleton can be characterized by the CC stretch/CH_3 rock coupled vibrations at 1092, 1065, 980, 953, and 852 cm^{-1} [31–33].

The β-CD FTIR spectrum (Figures 4(a) and 4(c)) is characterized by the intense broad band associated with the H_2O and the primary and secondary O–H stretching vibrations (3396 cm^{-1}), as well as the asymmetric C–H stretching vibration (2924 cm^{-1}). The absorption bands at 946, 937, 609, 577, and 530 cm^{-1} correspond to the glucopyranose ring vibrations [18, 34] and the last three are located in a relatively free zone of the FOS spectrum.

As presented in Figure 4(c), the FTIR spectrum of FOS/β-CD KP indicates that, in the spectral region of the O–H stretching vibrations, the band is shifted to 3390 cm^{-1}, as a consequence of the involvement of β-CD hydroxyl groups in other environment: position modifications of the water molecules, exclusion of β-CD intracavitary water, formation of new H-bonds [4, 9]. Nevertheless, the slight augmentation of the intensity in the kneaded product, in comparison with the physical mixture, may account for new H-bonds formed with the FOS molecule. The peaks at 3060 and 3086 cm^{-1}, corresponding to the C_{ar}–H stretching vibrations, are not detected in the physical mixture and the kneaded product, probably covered by the β-CD –OH stretching tail, but the most intense 3030 cm^{-1} band is present, although it is attenuated in intensity for FOS/β-CD KP in comparison with FOS/β-CD PM. The CH_3 (i-propyl, ethyl) stretching vibration is shifted to 2972 cm^{-1} in the kneaded product and diminished in comparison with the physical mixture. In Figure 4(b) the C=O stretching peak from FOS ester group is still present at 1759 cm^{-1} in FOS/β-CD PM, but it is shifted at 1753 cm^{-1} and strongly attenuated and broadened in FOS/β-CD KP, thus suggesting that hydrogen bonds with β-CD were established. Similar decreases and simultaneous broadenings in the absorption intensities of the amide and ester (asymmetric) C=O stretching vibrations are observed for the kneaded product, the latter peak being shifted to 1603 cm^{-1}. Such a shift to higher wavenumbers of

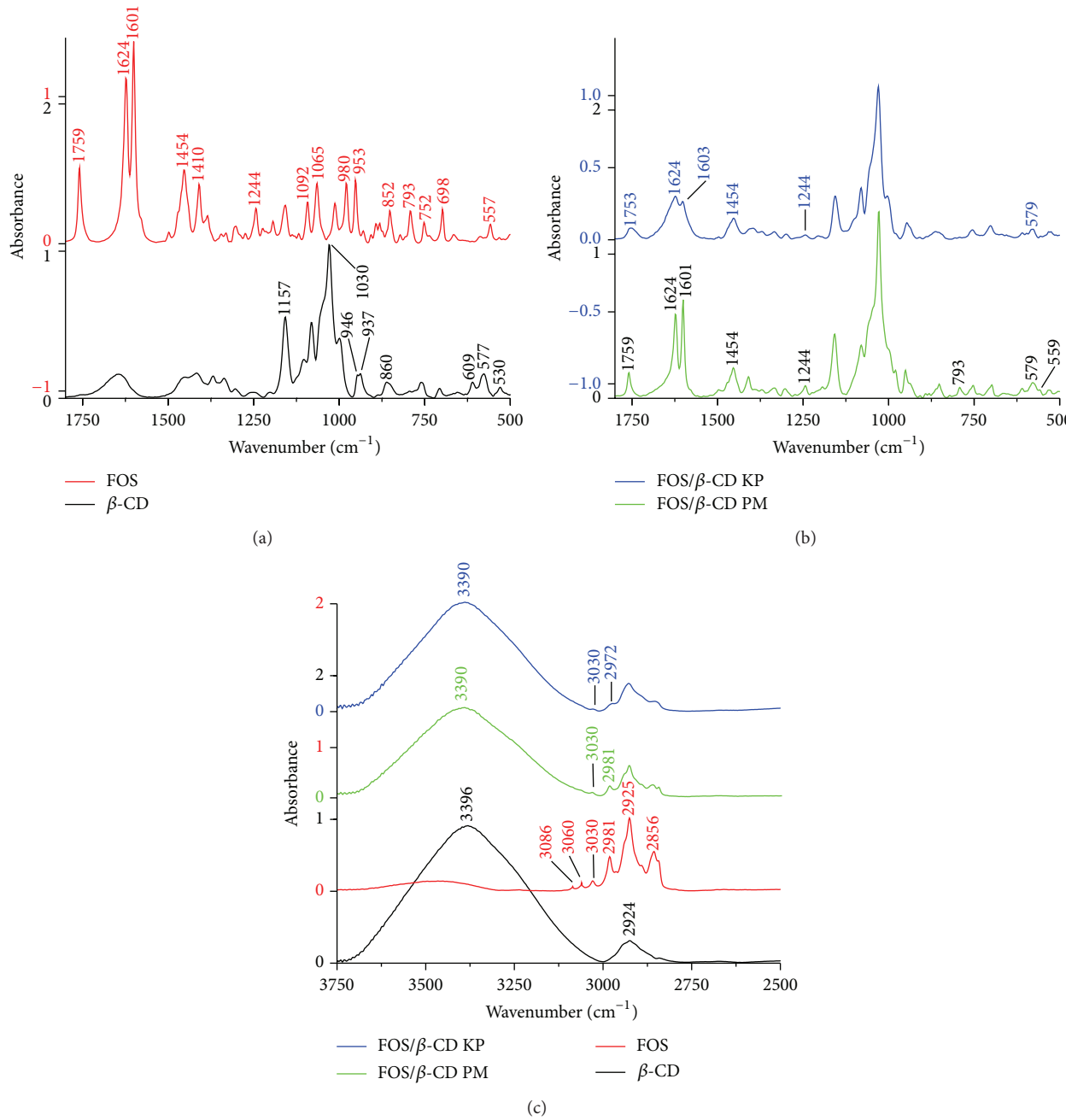

Figure 4: FTIR spectra of (a) FOS and β-CD in 2000–500 cm^{-1} spectral region, (b) FOS/β-CD physical mixture and FOS/β-CD kneaded product in 2000–500 cm^{-1} spectral region, and (c) β-CD, FOS, FOS/β-CD physical mixture and FOS/β-CD kneaded product in 4000–2500 cm^{-1} spectral region.

the carboxyl vibration was considered as evidence for the formation of the inclusion complex [35]. The band widening can be ascribed to the formation of hydrogen bonds with the cyclodextrin. A diminution of the proline C–N stretching intensity (1454 cm^{-1}) can also be detected for the supposed complex in comparison with the physical mixture. This also applies for the butyl CH_2 wagging (1244 cm^{-1}) and rocking (793 cm^{-1}) and for the aromatic out of plane (shifted at 559 cm^{-1}) vibrations. The CC stretch/CH_3 rock coupled vibration at 980 cm^{-1} is drastically diminished in FOS/β-CD KP but present in FOS/β-CD PM.

The intensity of the glucopyranose ring vibration (at 577 cm^{-1}) is shifted at 579 cm^{-1} in both binary systems and is clearly diminished in FOS/β-CD KP, thus demonstrating a mobility hindering for the cyclodextrin molecule; this is most likely due to the guest encapsulation.

The differences between the spectra of the kneaded product and the physical mixture, restrictions in vibrations, bends,

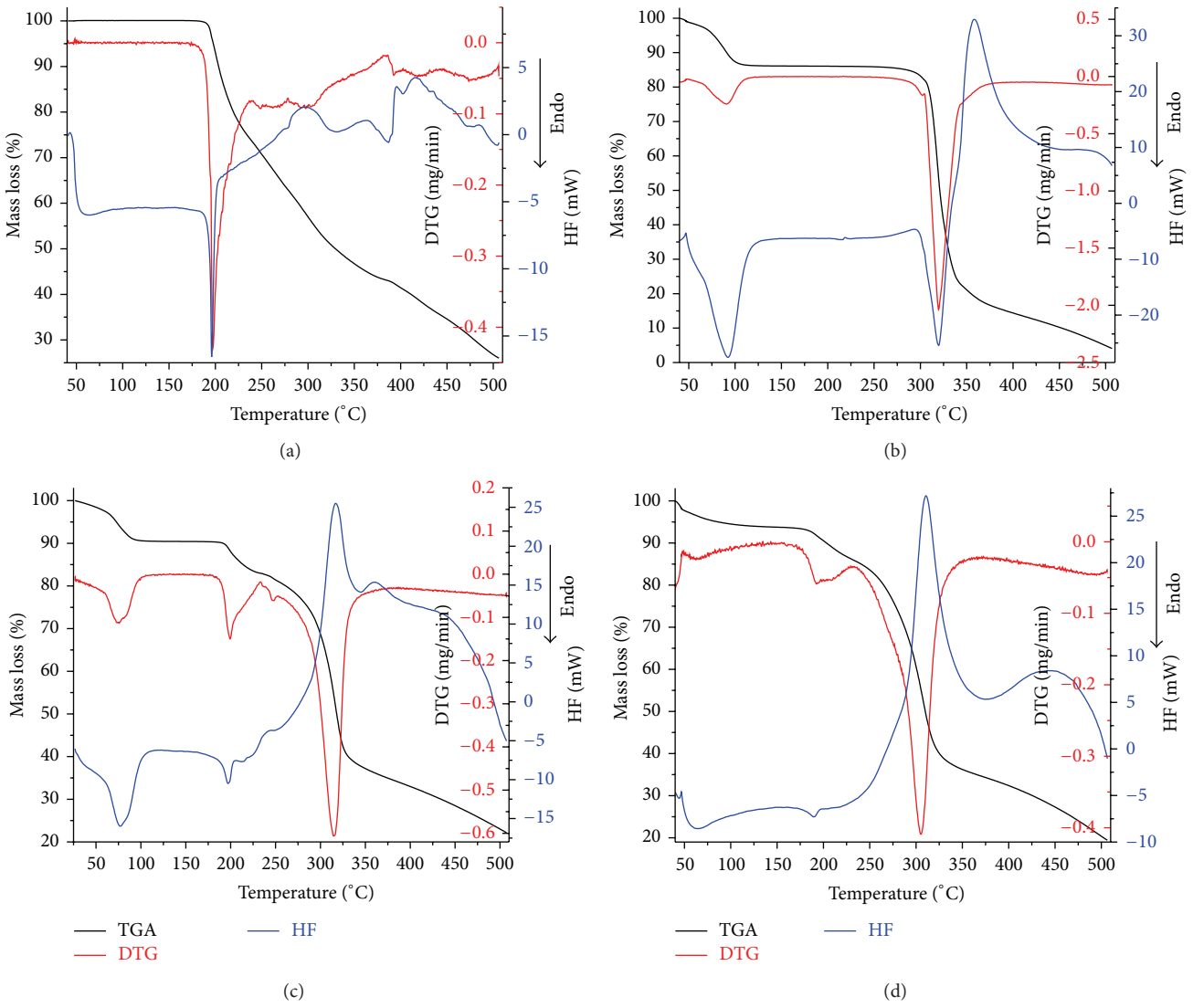

Figure 5: The thermal profile of (a) FOS, (b) β-CD, (c) FOS/β-CD physical mixture, and (d) FOS/β-CD kneaded product.

suggest that the former is a complex between FOS and β-CD. The spectra show that intermolecular interactions between the β-CD molecule and remote fragments (the ester, amide, and carboxyl groups, the isopropyl and ethyl substituents, the n-butyl chain, the proline, and the aromatic ring) of the FOS molecule are simultaneously influenced. Furthermore, it can be inferred from the spectra that the carbonyl and carboxyl groups are forming hydrogen bonds with the β-CD hydroxyls. This fact implies that these fragments and their neighborhoods are entirely or partially buried in the cavity of β-CD, because simultaneous H-bonds are possible, mainly with the β-CD primary hydroxyl groups. All these facts are proving the encapsulation of the guest molecule, that is, the existence of the inclusion complex.

Taking into account the deduced interactions between β-CD and FOS, involving distant parts of FOS and the results presented in Section 3.7, it cannot be excluded that complexes with favorable energies and different geometries are present in the kneaded product.

3.4. Thermal Analysis. The thermal profiles of the pure substances and their corresponding binary systems are provided in Figure 5.

The heat flow differential scanning calorimetry (HF) diagram discloses the FOS melting by a sharp endothermic peak at 196°C. The differential thermogravimetric (DTG) curve of pure FOS (Figure 5(a)) shows a sharp endothermic peak at 197.8°C, corresponding to the melting point of FOS, followed by the thermal degradation—a process that is confirmed by the thermogravimetric (TGA) curve.

The loss of water of β-CD is indicated by the TGA thermogram of β-CD (Figure 5(b)), which shows a small mass loss between 50°C and 130°C; the DTG and HF diagrams strengthen the β-CD dehydration process by its broad endothermic peaks having their maximum values at 91°C and 95°C, respectively. The melting point of β-CD has a higher value than FOS, as it is revealed at 319.6°C by the HF curve. There are no melting or other degradation processes of β-CD in the region of FOS melting.

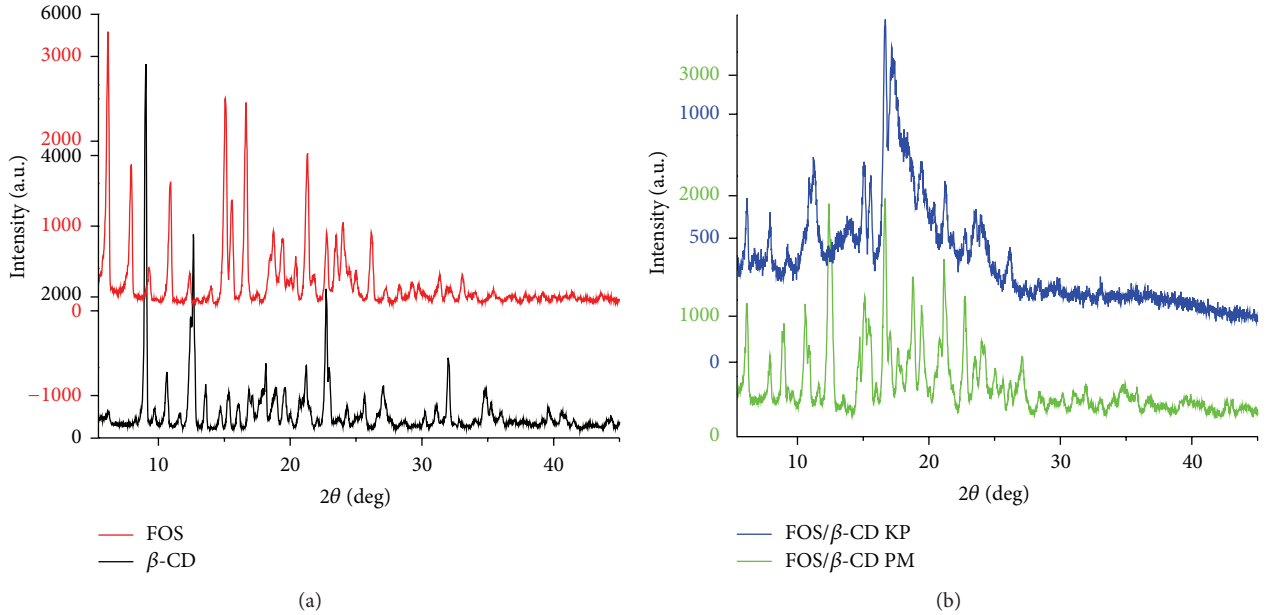

Figure 6: PXRD patterns of (a) FOS and β-CD and (b) their binary systems.

The TGA curve (Figure 5(c)) indicates a small mass loss for the FOS/β-CD physical mixture, corresponding to β-CD dehydration, and the DTG and HF curves point out that the corresponding endothermic peaks are shifted to lower temperatures at 74.2°C and 77°C in DTG and HF, respectively. The FOS melting, as indicated by the HF curve, is confirmed by the DTG curve, but the temperatures of the endothermic peaks are shifted to higher values with nearly 2°C for each curve in comparison with pure FOS. In the physical mixture, the melting temperature of β-CD—as shown in HF curve—appears at a lower value (i.e., 314.7°C).

The thermal profiles of the FOS/β-CD kneaded product (Figure 5(d)) indicate major differences in comparison with the FOS/β-CD physical mixture. The DTG and HF curves indicate that the dehydration endothermic peak of β-CD is highly reduced and shifted to a lower temperature (around 48°C); the HF curve indicates a significant peak reduction in terms of both maximum value and broadness. The TGA and DTG diagrams denote the decreasing of the FOS thermal stability in the FOS/β-CD kneaded product in comparison with the FOS alone (the degradation process starts at a lower temperature than FOS) thus indicating the changing of the thermal features after inclusion complex formation between FOS and β-CD. The HF curve also reveals the significant reduction and the displacement of the FOS distinctive melting endothermic peak (i.e., 185.4°C), which gives a hint about the crystallinity reduction of FOS along with the complexation. All these results are suggesting the inclusion of the FOS within the β-cyclodextrin cavity.

The TGA curve of FOS/β-CD KP (Figure 5(d)) presents a residue mass value of the sample at 119.2°C of 94.06% (Δm = 5.94%). However, at temperature T = 108.9°C, the residue mass of free β-CD (Figure 5(b)) is 86.50% (Δm = 13.50%). The difference of the Δm values for β-CD and FOS/β-CD KP corresponding to the first mass loss process from the TGA curves (recorded under the same heating rate of 10°C/min) is observed and can be explained by the fact that FOS, as a guest molecule, replaces the water molecules in the cavity of β-cyclodextrin, hence indicating the formation of an inclusion complex between β-CD and FOS.

Moreover, the shape of the FOS melting endotherm from the HF curves indicates that the free FOS is present in the kneaded product.

3.5. PXRD Analysis. Powder X-ray diffractometry is an appropriate procedure for establishing the molecular state of an inclusion complex [36].

The powder X-ray diffraction patterns of FOS, β-CD, FOS/β-CD physical mixture and FOS/β-CD kneaded product are depicted in Figure 6. The bulk FOS highly crystalline nature (Figure 6(a)) is highlighted by the sharp peaks at 6.16, 7.94, 10.92, 12.40, 15.08, 15.62, 16.64, 21.32 2θ [29]. The PXRD pattern of β-CD (Figure 6(a)) is characterized by sharp and distinctive peaks at 9.04, 12.64, 22.72, 31.98 2θ, which indicates its crystalline state. The XRD pattern of the FOS/β-CD physical mixture (Figure 6(b)) comprises all their characteristic diffraction peaks, being merely an overlap of the of FOS and β-CD XRD individual patterns, which therefore proves that there is minimum interaction between components.

The X-ray diffraction pattern of FOS/β-CD KP (Figure 6(b)) is not an overlapping of the individual FOS and β-CD XRD patterns anymore; conversely it presents a noticeable diminution of their characteristic sharp peaks, thus revealing a significant reduction of crystallinity. The FOS peaks intensities at 6.16 and 7.94 22θ are significantly reduced; at the same time the FOS diffraction peak at 10.92 2θ—which is reduced in FOS/β-CD physical mixture—is

Table 1: Heats of formation, kJ/mol, calculated with the PM3 method for the geometry optimized free host ($E_{\beta\text{-CD}}$), free guest (E_{FOS}), and complex (E_{compl}), respectively, and also the single point energy values for the host structure ($E_{\beta\text{-CD compl}}$) and guest structure ($E_{\text{FOS compl}}$), respectively, taken from the optimized complex geometry for the two possible forms (salt and ionic) of fosinopril and the three conformations taken to account for free FOS: (a) the nearest stable conformation to the crystal structure; (b) the global minimum energy conformation; (c) the nearest stable conformation to the FOS geometry in the complex; **1**, **2**, and **3** correspond to the three energy minima obtained by MM+ optimization.

Min	Form	$E_{\beta\text{-CD}}$	E_{FOS} (a)	E_{FOS} (b)	E_{FOS} (c)	E_{compl}	$E_{\beta\text{-CD compl}}$	$E_{\text{FOS compl}}$
1	COONa				−1790.29	−7958.69	−6094.07	−1778.24
2	COONa	−6095.50	−1793.36	−1859.43	−1786.44	−7942.88	−6078.99	−1780.79
3	COONa				−1828.14	−8108.27	−6055.86	−1717.76
1	COO^-				−1693.78	−7891.67	−6091.18	−1689.72
2	COO^-	−6095.50	−1667.52	−1741.00	−1697.11	−7922.78	−6071.46	−1685.99
3	COO^-				−1695.59	−8018.88	−6042.21	−1646.09

no longer present in FOS/β-CD KP diffraction pattern. On the other hand, new diffraction peaks at 11.20 and 17.16 2θ are observed in FOS/β-CD KP diffractogram, but not in FOS/β-CD PM. This indicates the changes in FOS and β-CD environment incurred by the kneading process. This outcome proves that the new compound is less crystalline than the drug, as it is entailed by the interaction between FOS and β-CD. These results emphasize the formation of a new amorphous solid phase in which FOS is no longer a crystalline substance, thus confirming the hypothesis of forming an FOS/β-CD inclusion complex.

3.6. Solubilization. The water solubility of the FOS/β-CD KP was appraised by preparing a concentrated solution [37]. The UV spectrophotometric measurements, achieved after an adequate dilution at 25°C, indicate that the water solubility of the included FOS is 9.4 mg/mL. A standard control experiment was performed by dissolving 27.6 mg of FOS/β-CD complex, in order to obtain a clear solution that is equivalent to 9.4 mg of FOS. The complexation with β-CD assures an aqueous molecular solution of FOS and hampers the hydrophobic interactions in water, which lead to self-association and micelle aggregates formation. These aggregates reduce the molecular effective concentration of FOS in water, hence incurring a negative impact on its bioavailability [38]. Thus, due to the complexation, the FOS water solubility is increased more than 6 times in comparison with the micelle occurrence threshold (which is about 1.5 mg/mL). This indicates that the solubility of the FOS/β-CD complex is adequate for tablet dosage form [37].

3.7. Molecular Modeling. The FOS molecule is a complex one, due to its geometry and its variety of functional groups. Therefore, it comes as no surprise that the procedure described in the experimental section, which identifies the preliminary global energy minimum for the binding energy, has resulted in three minima, labeled as **1**, **2**, and **3**, respectively. The corresponding geometrical structures, resulting from MM+ calculations were afterwards submitted to semiempirical PM3 calculations.

The experimental pKa of FOS lies between 4 and 5.1, even in alcohol-water mixtures [39], thus the contribution of the –COOH form, for the experimental conditions of the complex preparation, can be considered as quite negligible. From the FTIR data it can be concluded that the ionized carboxylate group is also present in the β-CD entrapped fosinopril molecule. In order to clarify the influence of the Na^+ ion, the PM3 geometry optimization for the three MM+ optimized structures was accomplished by evaluating both sodium salt and $-COO^-$ forms. In the subsequent calculations, which refer to the different types of energies belonging to the complexes, three types of free FOS conformations were used: (a) the nearest to the crystal structure, (b) the global minimum energy conformation, and (c) the nearest conformation to the FOS molecule already in the complex cavity. Conformations of types (a) and (c) were calculated by submitting the geometric structures of FOS from both the crystal and the optimized complex to the PM3 energy minimization process. Conformations of type (b) were obtained after searching the conformational space of the two species: salt and ionic. Only the PM3 optimized crystal geometry was used for the β-CD molecule, because the preserved intramolecular hydrogen-bonded array, formed by the primary hydroxyl groups, sufficiently stabilizes this structure.

The energy values for the free host molecule ($E_{\beta\text{-CD}}$), the free guest molecule (E_{FOS}) (for FOS the three mentioned conformations were involved), and the complex (E_{compl}) were obtained by performing full geometry optimizations for the starting structures with the PM3 method, without any geometrical or symmetry constraints. Using the frozen geometries of the host and the guest molecules as they are in the optimized complex, a PM3 single point run was performed in order to obtain $E_{\beta\text{-CD compl}}$ and $E_{\text{FOS compl}}$, that is, the energies corresponding to these molecules. Table 1 presents all these energies as heats of formation (kJ/mol).

These values allow for the calculation of the interaction energy for the complex (E_{interact}), the deformation energies of the host ($E_{\text{def }\beta\text{-CD}}$) and the guest ($E_{\text{def FOS}}$) from the complex, and the complexation (binding) energy (E_{bind}), respectively, using (2), (3), (4), and (5), which are expressed in kJ/mol within Table 2. They were calculated for the three

Table 2: The interaction, $E_{interact}$, deformation, $E_{def\ \beta\text{-CD}}$ (host, β-cyclodextrin), $E_{def\ FOS}$ (guest, fosinopril), E_{bind} binding energies (kJ/mol), and the charge on the β-CD molecule calculated for the three possible optimal geometries of the FOS/β-CD complex, using PM3 calculation results for the two possible forms (salt and ionic) of fosinopril and the three conformations taken to account for free FOS: (a) the nearest stable conformation to the crystal structure; (b) the global minimum energy conformation; (c) the nearest stable conformation to the FOS geometry in the complex; **1**, **2**, and **3** correspond to the three energy minima obtained by MM+ optimization.

Min	Form	$E_{interact}$	$E_{def\ \beta\text{-CD}}$	$E_{def\ FOS}$			E_{bind}			Charge β-CD
				(a)	(b)	(c)	(a)	(b)	(c)	(e^- units)
1	COONa	−86.38	1.44	15.12	81.18	12.05	−69.83	−3.76	−72.90	−0.0216
2	COONa	−83.10	16.51	12.57	78.63	5.65	−54.02	12.05	−60.94	−0.0426
3	COONa	−334.64	39.64	75.60	141.67	110.37	−219.40	−153.34	−184.63	+0.0670
1	COO^-	−110.77	4.32	−3.20	51.27	4.06	−109.65	−55.17	−102.39	−0.0359
2	COO^-	−165.37	24.05	0.56	55.04	11.16	−140.77	−86.29	−130.17	−0.0535
3	COO^-	−330.57	53.29	40.42	94.90	49.48	−236.86	−182.38	−227.80	−0.1593

possible optimal geometries of the FOS/β-CD complex, using PM3 calculation results for the two possible forms (salt and ionic) of FOS and the three energy minima obtained by MM+ optimization, corresponding to (a), (b), and (c) FOS conformations:

$$E_{interact} = E_{compl} - \left(E_{\beta\text{-CD compl}} + E_{FOS\ compl}\right), \quad (2)$$

$$E_{def\ \beta\text{-CD}} = E_{\beta\text{-CD compl}} - E_{\beta\text{-CD}}, \quad (3)$$

$$E_{def\ FOS} = E_{FOS\ compl} - E_{FOS}, \quad (4)$$

$$E_{bind} = E_{compl} - \left(E_{\beta\text{-CD}} + E_{FOS}\right). \quad (5)$$

The inspection of the energy values from Table 2 reveals the following observations.

(i) All the interaction energies are favorable, the highest values being those corresponding to minimum **3**. The smallest value is presented by the COONa **2** complex.

(ii) As expected, the deformation energies for β-CD are smaller than those corresponding to column (b) $E_{def\ FOS}$. Also, if in the complex preparation procedure there are conditions so that the FOS molecule takes the conformation corresponding to the global minimum (hydrophobic stacking structure, similar to that of Liu et al. [27]), then the binding energies are smaller. Most probably, the paste consistency of the environment during the applied kneading method rather provides availability conditions for conformations corresponding to columns (a) or (c).

(iii) The FOS deformation energies in the case of minimum **3** are quite high, but this is not an unusual situation (e.g., the case of miconazole [40]). The high flexibility can be decisive in the stability of cyclodextrin complexes [41].

(iv) For all situations, except E_{bind} **2**(b) COONa, the negative binding energy values obtained suggest that the inclusion is an enthalpy-driven favorable process. The most pronounced effect is displayed for complex structure **3**.

(v) The results globally revealed that complexes formed with the FOS which present the COO^- anion are more stable than the COONa complexes. This finding is in accordance with the observations from [42] and references therein.

For a more detailed analysis, more calculated or inferred data are used. These data are directed to the principally accepted driving forces of complex formation: hydrogen bonding, charge-transfer, and van der Waals interactions [43, 44]. The hydrophobic interaction cannot be considered here, as the theoretical calculations are performed in vacuum.

Thus, a careful structure analysis for these complexes (which are presented in Figure 7) was performed, in order to deliver the data from Table 3. The hydrogen bonds, O–H···O, are classified according to Steiner [44], the criterions being the H···O, O–H, and O···O distances and the O–H···O angle. Steiner's "moderate hydrogen bonds" are named "strong hydrogen bonds" by Desiraju and Steiner [45]. The van der Waals interactions are highlighted when the distances between the atoms are equal or 20% smaller than the sum of van der Waals radii. In Figure 7 only the COONa type complexes are presented, but Table 3 contains the data for all the analyzed complexes.

The hydrogen bonds contribution to the intermolecular binding energy is less than 16-17 kJ/mol for the weak hydrogen bonds; at the same time, it is between 16–62 kJ/mol for the moderate ones [44, 45]. Jurema and Shields [46] stated that the PM3 method predicts the energy of intermolecular H-bonds in reasonable agreement with their energy behavior, but underestimating somewhat the real heats of association. Taking into account these facts and analyzing the number and the quality of hydrogen bonds in the stable complex structures (Figures 7(a), 7(c), and 7(e) and Table 3), together with the E_{bind} values (Table 2), one can conclude that, besides the H-bonds, there are also other interaction energies to be considered in the stabilization of the complexes.

Regarding the charge transferred between the host and guest molecules, the last column of Table 2 presents the electronic charge on the cyclodextrin molecule in the complex. In all cases, except the COONa **3** complex, the electron acceptor molecule is β-CD. In this last case, a charge transfer appears toward the FOS molecule, most probably because the Na ion is inside the cyclodextrin cavity. From the three Na containing complexes, the lowest lying LUMO is displayed

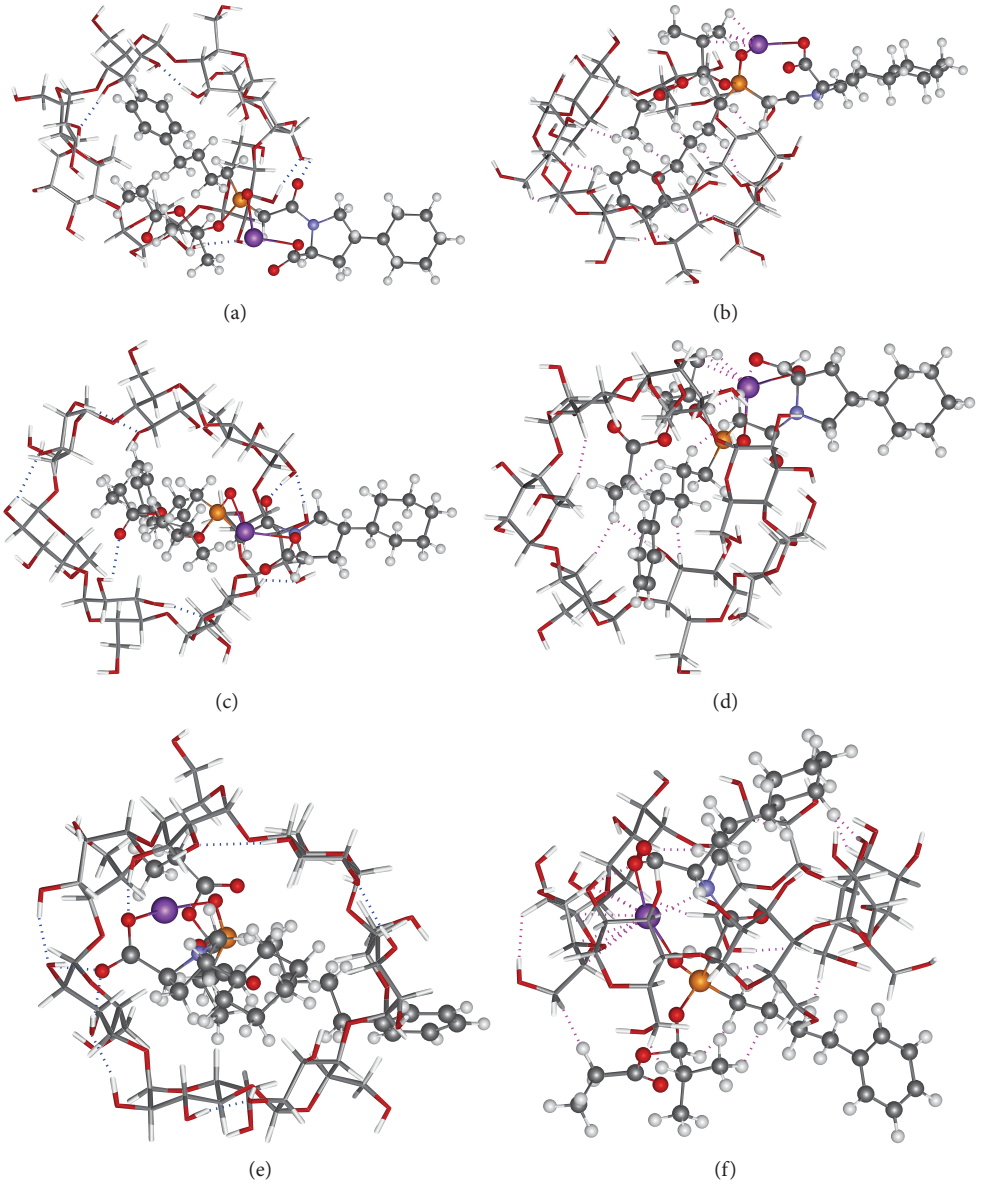

FIGURE 7: Structure views of the FOS/β-CD complexes with the Na salt form of fosinopril: hydrogen bond interactions (blue dashed lines) (a), (c), and (e) and van der Waals interactions (magenta dashed lines) (b), (d), and (f) for COONa type complexes **1**, **2**, and **3**, respectively.

by **3** (**1**: −0.54 eV, **2**: −0.46 eV, and **3**: −1.00 eV). On the other hand, by analyzing the charges on the FOS in complex **3** in comparison with the free FOS, an exceeding charge can be found especially on the atoms substantially participating in LUMO. Thus, this calculated charge transfer in the COONa **3** complex is fully justified. The stability order from Table 2 (see E_{bind}) is **3** > **1** > **2** for COONa and **3** > **2** > **1** for COO^- complexes, respectively. For the COO^- complexes the order is confirmed by the charge transferred between the molecules, but not for the COONa complexes. In this context, the van der Waals interactions had to be also analyzed.

In Figures 7(b), 7(d), and 7(f) and Table 3 the potential van der Waals interactions between the FOS and β-CD molecules for the three types of complexes are highlighted. The poorest in van der Waals contacts is complex **2**, which contains the COONa form of the FOS molecule; this justifies the smallest host-guest binding capacity for this complex and, at the same time, reveals the importance of this type of interaction for the stability of the complexes. The richest van der Waals interaction networks are present in complexes corresponding to minimum **3**, which also exhibit the highest stability according to our calculations.

By analyzing Tables 2 and 3 it can be inferred that the complexation process involves, besides H-bonds, van der Waals and charge transfer interactions too. Moreover, the H-bond behavior reveals that the strongest H-bond interactions are set in type **3** complexes. These arguments suggest that the most stable FOS/β-CD complexes are of type **3**.

The molecular modeling outcomes are in agreement with the experimental findings afforded by the FTIR spectra.

Table 3: Hydrogen bonds and the most important van der Waals interactions between FOS and β-CD, for each complex type, as resulting from PM3 calculations.

Min	Form	Interactions FOS-βCD in complex
1	COONa	(i) 2 weak H-bonds secondary OH$\cdots$O=C amide (ii) vdW contacts: $C_6H_5(CH_2)_4$ with the H-3′ and H-5′β-CD, as for enalapril in [24]
2	COONa	(i) 1 moderate and 1 weak H-bond secondary OH$\cdots$O=C amide and ester, respectively (ii) vdW contacts: $(CH_2)_4$, CH_3(Et) with H-3′β-CD
3	COONa	(i) 3 moderate H-bonds secondary OH$\cdots$OOC carboxyl (ii) vdW contacts: cyclohexyl CH_2, prolyl CH and (N)CH_2, (P)CH_2(C=O) with H-3′ and H-5′β-CD, and CH_2(Et), CH i-Pr with (C)H_2-6′β-CD
1	COO^-	(i) 2 weak H-bonds secondary OH$\cdots$O=C amide (ii) vdW contacts: $C_6H_5(CH_2)_4$, CH_3(Et) with the H-3′ and H-5′β-CD
2	COO^-	(i) 1 moderate and 1 weak H-bond secondary OH$\cdots$O=C amide and ester, respectively (ii) vdW contacts: $C_6H_5(CH_2)_4$ interactions with H-3′ and H-5′, and (C)H_2-6′β-CD, and between CH_3(Et) and H-3′, H-5′β-CD
3	COO^-	(i) 4 moderate H-bonds secondary OH$\cdots$OOC carboxyl (ii) vdW contacts: $(C_6H_5)CH_2$, prolyl CH and (N)CH_2, (P)CH_2(C=O) with H-3′ and H-5′β-CD, and CH_2(Et), CH i-Pr, $C_6H_5CH_2$ with (C)H_2-6′β-CD

All the IR absorbance values and corresponding molecular fragments affected by the guest inclusion phenomenon are mirrored in the molecular interactions exhibited by the theoretical results: H-bonds formation, close contacts hindering the different type of vibrations identified as modified in the spectra by the inclusion complex formation. In addition, the structures corresponding to the three types of stable host-guest complexes, delivered by the molecular modeling study, are endorsing the result suggested by the infrared spectra, concerning the existence of a mixture of complexes. The stoichiometry determination leads to the conclusion that a 1 : 1 type complex is formed. The IR spectra demonstrate the simultaneous existence of hydrogen bonds between β-CD OH and three FOS fragments: the COO group, the amide, and the ester C=O. The calculated minimum energy structures show that this is possible only if in the experimentally analyzed KP probe there are simultaneously at least molecules of type **2** and **3** present. The strongly affected CH_2 wagging and rocking (most probably corresponding to the C_4 aliphatic chain) and aromatic out of plane vibrations suggest the presence of type **1** complex. Nonetheless the calculated E_{bind} values indicate that structure **3** probably dominates within the proposed mixture.

Figure 7 illustrates the structures of FOS/β-CD complexes with the Na salt of fosinopril, which confirm the spectral data from Section 3.3, regarding the involvement of different FOS groups in the complexation process with β-CD.

4. Conclusions

The usage of cyclodextrins is a valuable technique for increasing the stability and the bioavailability of the included drugs. As such, this paper reports the interaction between FOS and β-CD, by experimental and theoretical approaches. The experimental results indicated that a real inclusion complex was formed between FOS and β-CD when the kneading preparation method was applied, with a 1 : 1 stoichiometry, as determined by Job's technique. The stability constant of FOS/β-CD was obtained as 278.93 M^{-1}, by employing the Benesi-Hildebrand method. FTIR, thermal analysis, and PXRD were used for confirming inclusion complex formation. The FTIR data correlated with molecular modeling results endorse the FOS/β-CD inclusion complex formation. The established stoichiometry and the FTIR analysis, together with the molecular modeling results, suggest that the kneaded product is a mixture of complexes with three different stable molecular structures. The theoretical energy calculations indicate that the dominant structure should be that with the carboxyl, P=O, amide, and proline groups buried in the β-CD cavity.

Conflict of Interests

The authors declare that there is no conflict of interests regarding the publication of this paper.

Acknowledgment

The authors are grateful to Professor Mircea Mracec from the Institute of Chemistry Timişoara of the Romanian Academy, for providing access to the HyperChem 7.5 software package.

References

[1] M. E. Davis and M. Brewster, "Cyclodextrin-based pharmaceutics: past, present and future," *Nature Reviews Drug Discovery*, vol. 3, pp. 1023–1035, 2004.

[2] T. Irie and K. Uekama, "Pharmaceutical applications of cyclodextrins. III. Toxicological issues and safety evaluation," *Journal of Pharmaceutical Sciences*, vol. 86, no. 2, pp. 147–162, 1997.

[3] J. Szejtli, "Past, present and futute of cyclodextrin research," *Pure and Applied Chemistry*, vol. 76, no. 10, p. 1825, 2004.

[4] M. Brewster and T. Loftsson, "Cyclodextrins as pharmaceutical solubilizers," *Advanced Drug Delivery Reviews*, vol. 59, no. 7, pp. 645–666, 2007.

[5] J. B. Kostis, W. Thomas Garland, C. Delaney, J. Norton, and W.-C. Liao, "Fosinopril: pharmacokinetics and pharmacodynamics in congestive heart failure," *Clinical Pharmacology and Therapeutics*, vol. 58, no. 6, pp. 660–665, 1995.

[6] V. Ranade and J. C. Somberg, "Rapid determination of partition coefficients between n-octanol/water for cardiovascular therapies," *The American Journal of Therapeutics*, vol. 9, no. 1, pp. 19–24, 2002.

[7] M. Remko, "Acidity, lipophilicity, solubility, absorption, and polar surface area of some ACE inhibitors," *Chemical Papers*, vol. 61, no. 2, pp. 133–141, 2007.

[8] European Pharmacopoeia, *Monograph of Fosinopril Sodium*, vol. 2073, European Pharmacopoeia, 7th edition, 2011.

[9] I. Bratu, I. Kacso, G. Borodi, D. E. Constantinescu, and F. Dragan, "Inclusion compound of fosinopril with β-cyclodextrin," *Spectroscopy*, vol. 23, no. 1, pp. 51–58, 2009.

[10] T. Loftsson and M. E. Brewster, "Pharmaceutical applications of cyclodextrins: basic science and product development," *Journal of Pharmacy and Pharmacology*, vol. 62, no. 11, pp. 1607–1621, 2010.

[11] Z. Wang, K. Morris, and B. Chu, "Aggregation behavior of fosinopril sodium—a new angiotensin-converting enzyme inhibitor," *Journal of Pharmaceutical Sciences*, vol. 84, pp. 609–613, 1995.

[12] T. Loftsson and D. Duchene, "Cyclodextrins and their pharmaceutical applications," *International Journal of Pharmaceutics*, vol. 329, no. 1-2, pp. 1–11, 2007.

[13] A. B. Thakur, K. Morris, J. A. Grosso et al., "Mechanism and kinetics of metal ion-mediated degradation of fosinopril sodium," *Pharmaceutical Research*, vol. 10, no. 6, pp. 800–809, 1993.

[14] L. Sbârcea, L. Udrescu, L. Drăgan, C. Trandafirescu, Z. Szabadai, and M. Bojiță, "Thin-layer cromatography analysis for inclusion complexes of fosinopril and zofenopril with cyclodextrins," *Farmacia*, vol. 58, no. 4, pp. 478–484, 2010.

[15] L. Sbarcea, L. Udrescu, L. Dragan et al., "Characterization of fosinopril natrium-hydroxypropyl-β-cyclodextrin inclusion complex," *Revista de Chimie*, vol. 62, no. 3, pp. 349–351, 2011.

[16] L. Sbârcea, L. Udrescu, L. Drăgan, C. Trandafirescu, Z. Szabadai, and M. Bojiță, "Fosinopril-cyclodextrin inclusion complexes: phase solubility and physicochemical analysis," *Die Pharmazie*, vol. 66, no. 8, pp. 584–589, 2011.

[17] W. Misiuk and M. Zalewska, "Investigation of inclusion complex of trazodone hydrochloride with hydroxypropyl-β-cyclodextrin," *Carbohydrate Polymers*, vol. 77, no. 3, pp. 482–488, 2009.

[18] J. S. Negi and S. Singh, "Spectroscopic investigation on the inclusion complex formation between amisulpride and γ-cyclodextrin," *Carbohydrate Polymers*, vol. 92, no. 2, pp. 1835–1843, 2013.

[19] H. A. Benesi and J. H. Hildebrand, "A spectrophotometric investigation of the interaction of iodine with aromatic hydrocarbons," *Journal of the American Chemical Society*, vol. 71, no. 8, pp. 2703–2707, 1949.

[20] N. Anderson, D. Lust, K. Colapret, J. Simpson, M. Malley, and J. Gougoutas, "Sulfonation with inversion by Mitsunobu reaction: an improvement on the original conditions," *The Journal of Organic Chemistry*, vol. 61, no. 22, pp. 7955–7958, 1996.

[21] "Cambridge Crystallographic Data Centre code: TUHMOY," http://www.ccdc.cam.ac.uk/pages/Home.aspx.

[22] R. W. Seidel and B. B. Koleva, "B-Cyclodextrin 10.41-hydrate," *Acta Crystallographica Section E*, vol. 65, no. 12, pp. o3162–o3163, 2009.

[23] "Cambridge Crystallographic Data Centre code: SUJDAD," http://www.ccdc.cam.ac.uk/pages/Home.aspx.

[24] S. Khan, K. Fatma, and S. Ali, "A comparative study of complexation of enalapril with α-, β- and γ-cyclodextrins in aqueous medium: structure elucidation of inclusion complexes using NMR spectroscopic and molecular mechanics methods," *Journal of Inclusion Phenomena and Macrocyclic Chemistry*, vol. 72, no. 3-4, pp. 413–421, 2012.

[25] L. Liu and Q.-X. Guo, "Use of quantum chemical methods to study cyclodextrin chemistry," *Journal of Inclusion Phenomena and Macrocyclic Chemistry*, vol. 50, no. 1-2, pp. 95–103, 2004.

[26] C. Yan, Z. Xiu, X. Li, and C. Hao, "Molecular modeling study of β-cyclodextrin complexes with (+)-catechin and (−)-epicatechin," *Journal of Molecular Graphics and Modelling*, vol. 26, pp. 420–428, 2007.

[27] S. Liu, Y. Shi, Q. Zhang, and G. Song, "Conformational study of fosinopril sodium in solution using NMR and molecular modeling," *Magnetic Resonance in Chemistry*, vol. 41, no. 8, pp. 609–614, 2003.

[28] E. Brothers, "Sodium parameters for AM1 and PM3 optimized using a modified genetic algorithm," *The Journal of Physical Chemistry B*, vol. 106, no. 10, pp. 2779–2785, 2002.

[29] H. G. Brittain, K. R. Morris, D. E. Bugay, A. B. Thakur, and A. T. M. Serajuddin, "Solid-state NMR and IR for the analysis of pharmaceutical solids: polymorphs of fosinopril sodium," *Journal of Pharmaceutical and Biomedical Analysis*, vol. 11, no. 11-12, pp. 1063–1069, 1993.

[30] A. Barth and C. Zscherp, "What vibrations tell us about proteins," *Quarterly Reviews of Biophysics*, vol. 35, no. 4, pp. 369–430, 2002.

[31] N. Colthup, *Introduction to Infrared and Raman Spectroscopy*, Elsevier, San Diego, Calif, USA, 2nd edition, 2012.

[32] J. C. Amicangelo, B. Golec, M. Bahou, and Y.-P. Lee, "Infrared spectrum of the 2-chloroethyl radical in solid para-hydrogen," *Physical Chemistry Chemical Physics*, vol. 14, no. 2, pp. 1014–1029, 2012.

[33] C. Y. Panicker, H. T. Varghese, and L. Ushakumary, "IR, Raman and SERS spectra of ethyl salicylate," *Journal of Raman Spectroscopy*, vol. 40, no. 12, pp. 2023–2030, 2009.

[34] R. C. Sabapathy, S. Bhattacharyya, W. E. Cleland Jr., and C. L. Hussey, "Host-guest complexation in self-assembled monolayers: inclusion of a monolayer-anchored cationic ferrocene-based guest by cyclodextrin hosts," *Langmuir*, vol. 14, no. 14, pp. 3797–3807, 1998.

[35] N. V. Roik and L. A. Belyakova, "Thermodynamic, IR spectral and X-ray diffraction studies of the "β-cyclodextrin-para-aminobenzoic acid" inclusion complex," *Journal of Inclusion Phenomena and Macrocyclic Chemistry*, vol. 69, no. 3-4, pp. 315–319, 2011.

[36] Z. Aigner, O. Berkesi, G. Farkas, and P. Szabó-Révész, "DSC, X-ray and FTIR studies of a gemfibrozil/dimethyl-β-cyclodextrin inclusion complex produced by co-grinding," *Journal of Pharmaceutical and Biomedical Analysis*, vol. 57, no. 1, pp. 62–67, 2012.

[37] S. Ma, W. Chen, X. Yang et al., "Alpinetin/hydroxypropyl-β-cyclodextrin host–guest system: preparation, characterization, inclusion mode, solubilization and stability," *Journal of Pharmaceutical and Biomedical Analysis*, vol. 67-68, pp. 193–200, 2012.

[38] D. K. Clodfelter, A. H. Pekar, D. M. Rebhun et al., "Effects of non-covalent self-association on the subcutaneous absorption of a therapeutic peptide," *Pharmaceutical Research*, vol. 15, no. 2, pp. 254–262, 1998.

[39] M. Popović, G. Popović, and D. Agbaba, "The effects of anionic, cationic, and nonionic surfactants on acid-base equilibria of ACE inhibitors," *Journal of Chemical & Engineering Data*, vol. 58, no. 9, pp. 2567–2573, 2013.

[40] V. Barillaro, G. Dive, P. Bertholet et al., "Theoretical and experimental investigations on miconazole/cyclodextrin/acid complexes: Molecular modeling studies," *International Journal of Pharmaceutics*, vol. 342, no. 1-2, pp. 152–160, 2007.

[41] M. V. Rekharsky and Y. Inoue, "Complexation thermodynamics of cyclodextrins," *Chemical Reviews*, vol. 98, no. 5, pp. 1875–1917, 1998.

[42] Y. Fu, L. Liu, and Q.-X. Guo, "A theoretical study on the inclusion complexation of cyclodextrins with inorganic cations and anions," *Journal of Inclusion Phenomena and Macrocyclic Chemistry*, vol. 43, pp. 223–229, 2002.

[43] L. Liu and Q.-X. Guo, "The driving forces in the inclusion complexation of cyclodextrins," *Journal of Inclusion Phenomena and Macrocyclic*, vol. 42, no. 1-2, pp. 1–14, 2002.

[44] T. Steiner, "The hydrogen bond in the solid state," *Angewandte Chemie International Edition*, vol. 41, no. 1, pp. 48–76, 2002.

[45] G. Desiraju and T. Steiner, *The Weak Hydrogen Bond: In Structural Chemistry and Biology*, Oxford University Press, 2001.

[46] M. W. Jurema and G. C. Shields, "Ability of the PM3 quantum-mechanical method to model intermolecular hydrogen bonding between neutral molecules," *Journal of Computational Chemistry*, vol. 14, no. 1, pp. 89–104, 1993.